Functional Analysis of a Juvenile Hormone Inducible Transcription Factor, Krüppel homolog 1, in the Bean Bug, Riptortus pedestris

AUTHOR(S):

Dong, Li; Muramatsu, Nobuki; Numata, Hideharu; Ito, Chihiro

CITATION:

Dong, Li ...[et al]. Functional Analysis of a Juvenile Hormone Inducible Transcription Factor, Krüppel homolog 1, in the Bean Bug, Riptortus pedestris. Zoological Science 2022, 39(6): 562-569

ISSUE DATE:

2022-12

URL:

http://hdl.handle.net/2433/286100

Functional Analysis of a Juvenile Hormone Inducible Transcription Factor, Krüppel homolog 1, in the Bean Bug, Riptortus pedestris

Authors: Dong, Li, Muramatsu, Nobuki, Numata, Hideharu, and Ito, Chihiro

Source: Zoological Science, 39(6) : 562-569

Published By: Zoological Society of Japan

URL: https://doi.org/10.2108/zs220025

ZOOLOGICAL SCIENCE **39**: 562–569 (2022)

Functional Analysis of a Juvenile Hormone Inducible Transcription Factor, Krüppel homolog 1, in the Bean Bug, *Riptortus pedestris*

Li Dong[1], Nobuki Muramatsu[1], Hideharu Numata[1], and Chihiro Ito[1,2*]

[1]*Graduate School of Science, Kyoto University, Sakyo, Kyoto 606-8502, Japan*
[2]*Department of Biochemistry, Faculty of Pharmacy, Osaka Medical and Pharmaceutical University, 4-20-1 Nasahara, Takatsuki, Osaka 569-1094, Japan*

Juvenile hormone (JH) has two major functions in insects, i.e., suppression of metamorphosis in the larval or nymphal stage and promotion of reproduction in the adult stage. Krüppel homolog 1 (Kr-h1), a C_2H_2 zinc-finger type transcription factor, is reported to act downstream of the JH receptor complex. In the present study, the function of Kr-h1 was examined in adults and nymphs of *Riptortus pedestris* by RNA interference (RNAi). After injection of adults with dsRNA of *Kr-h1*, the expression level of *Kr-h1* was significantly decreased in the abdomen. *Kr-h1* dsRNA-injection resulted in a lower proportion of individuals with developed ovaries, but the difference was not statistically significant. The transcript levels of *cyanoprotein-α* and *vitellogenin-1*, which are JH-inducible genes encoding yolk proteins, were not affected in the abdomen by *Kr-h1* knockdown. *Kr-h1* dsRNA-injection was effective for suppression of *Kr-h1* expression in nymphs. Some *Kr-h1* dsRNA-injected fifth (final) instar nymphs had morphological defects in the wing bud. Moreover, they had several adult morphological features, including ocelli in the head, connexivum in the abdomen, coloring of the dorsal abdomen, and genitals. The nymphs possessing adult features did not emerge as adults during 1 month. These results demonstrated that Kr-h1 is necessary for maintaining nymphal characters in *R. pedestris*. The function of Kr-h1 in ovarian development remains unclear in *R. pedestris*.

Key words: juvenile hormone, ovarian development, JH-inducible gene, *cyanoprotein*, *vitellogenin*, precocious metamorphosis, RNAi

INTRODUCTION

Juvenile hormone (JH), a sesquiterpenoid hormone secreted from the corpus allatum, is one of the major hormones that control insect development, metamorphosis, and reproduction (Jindra et al., 2013; Roy et al., 2018). In adults of both most hemimetabolous and some holometabolous insects, JH plays a principal role as a gonadotropic hormone to provoke vitellogenesis, i.e., accumulation of yolk proteins during oogenesis. Most insects synthesize vitellogenin (Vg) as a major yolk protein precursor in the fat body and finally deposit it in the oocyte (Wu et al., 2021). Vg is critical for egg maturation and, not surprisingly, downregulation of *Vg* by RNAi leads to decreased egg production (Lee et al., 2017). Krüppel homolog 1 (Kr-h1), encoded by JH-inducible *Kr-h1*, is a C_2H_2 zinc-finger type transcription factor and a key player in the JH signaling pathway initiated from the JH receptor complex composed of Methoprene-tolerant (Met) and Taiman (Tai) (Minakuchi et al., 2009; Roy et al., 2018; Jindra et al., 2021). The function of Kr-h1 has been examined by RNA interference (RNAi) for *Kr-h1* in several insect species. The roles of Kr-h1 in reproduction are not consistent among insect species: Kr-h1 plays pivotal roles in vitellogenesis in some species, such as *Locusta migratoria*, *Nilaparvata lugens*, *Bactrocera dorsalis*, *Sogatella furcifera*, and *Tribolium castaneum* (Song et al., 2014; Lin et al., 2015; Jiang et al., 2017; Yue et al., 2018; Hu et al., 2020; Naruse et al., 2020), but not in others, including two heteropterans, *Pyrrhocoris apterus* and *Cimex lectularius* (Smykal et al., 2014; Gujar and Palli, 2016).

On the other hand, Kr-h1 consistently plays an indispensable role in larval (nymphal) development and metamorphosis: Kr-h1 has been shown to be involved in maintaining the larval state in both hemimetabolous and holometabolous insects (Minakuchi et al., 2009; Konopova et al., 2011; Lozano and Belles, 2011; Ishimaru et al., 2019). In *P. apterus,* the downregulation of *Kr-h1* in fourth (penultimate) instar nymphs resulted in precocious development of the adult color pattern, wings, and genitals (Konopova et al., 2011). In *T. castaneum*, knockdown of *Kr-h1* in larvae caused precocious larval-pupal transition (Minakuchi et al., 2009; Ureña et al., 2016). Similar results were obtained in *Blattella germanica* and *Gryllus bimaculatus* (Lozano and Belles, 2011; Ishimaru et al., 2019).

The bean bug, *Riptortus pedestris*, is one of the representative species in Heteroptera in which physiological and endocrinological findings regarding JH have been accumu-

* Corresponding author. E-mail: chihiro.ito@ompu.ac.jp
doi:10.2108/zs220025

lated. In this species, ovarian development was shown to be regulated by JH (Numata and Hidaka, 1984), although the downstream pathway to vitellogenesis and ovarian development is unclear. Cyanoprotein-α (CP-α) and vitellogenin-1 (Vg-1) accumulate in eggs under reproductive conditions. In addition, the expression of their encoding genes and *Kr-h1* is induced by JH analog (Miura et al., 1991; Hirai et al., 1998; Ikeno et al., 2010; Dong et al., 2021). In the present study, we examined the function of Kr-h1, which is a candidate as a mediator of the pathway downstream of JH, by performing RNAi-mediated knockdown of *Kr-h1* in both adults and fourth instar nymphs of *R. pedestris*. We examined ovarian development and transcript levels of *CP-α* and *Vg-1* in adult females and observed the morphology of fifth (final) instar nymphs.

MATERIALS AND METHODS

Insects

Adults of *R. pedestris* were collected in Kyoto City (35.0°N, 135.8°E) from May to September in 2016–2018. Their progeny were used for experiments under long-day conditions of 16-h light and 8-h darkness (light 09:00–01:00, JST) at 25 ± 1°C, under which insects become reproductive. They were fed soybean grain and water containing 0.05% sodium ascorbate and 0.025% L-cysteine (Kamano, 1991).

Reproductive status

To examine the reproductive status, female adults were dissected in saline (0.9% NaCl solution) under a stereoscopic microscope. Females were classified as being reproductive or non-reproductive based on ovarian development, i.e., ovaries with light-blue yolk deposition in the oocytes were judged to be developed, whereas those with no deposition were judged to be undeveloped (Numata and Hidaka, 1982; Hafeez et al., 2020).

Sample preparation

Adult abdomens were collected individually before and after observation of the reproductive status. To examine gene expression in the fat body, the abdomen was collected because the majority of the fat body is located in the abdomen (Raikhel et al., 1997). Whole bodies were used for the analysis of gene expression in the fifth instar nymphs because of the small body size. All samples were individually stored in TRIzol Reagent (Life Technologies, Foster City, CA, USA) at –80°C until they were used for RNA extraction.

RNA extraction and cDNA synthesis

Total RNA was isolated using TRIzol Reagent according to the supplier's instructions. Genomic DNA was eliminated using DNase (Deoxyribonuclease I, Amplification Grade, Invitrogen, Waltham, USA). After DNase treatment, cDNA was synthesized from 1 μg of total RNA with a High Capacity cDNA Reverse Transcription Kit (Applied Biosystems, Foster City, USA). The cDNA was stored at –20°C until use.

RNAi

cDNA was used to synthesize *Kr-h1* double-stranded RNA (dsRNA). As a control, dsRNA of *β-lactamase* (*bla*), a gene that provides bacteria with ampicillin resistance, was also synthesized using the pGEX4T-1 vector (GE Healthcare, Chicago, USA). To obtain the T7 promoter-attached DNA fragment, cDNA or pGEX4T-1 vector was used as a template for PCR with KOD-plus ver.2 (TOYOBO, Osaka, Japan) according to the supplier's instructions. Primers used in reactions are listed in Table 1. The double-stranded RNAs (dsRNAs) were synthesized by using the T7 Ribomax Express RNAi System (Promega, Madison, USA) according to the supplier's instructions. The dsRNAs were dissolved in saline solution and stored at –20°C until use. To examine the function of *Kr-h1* in metamorphosis, fourth instar nymphs were injected with 1 μl of *Kr-h1* or *bla* dsRNA (3 μg/μl) into the abdomen on the day after the third nymphal ecdysis. To verify the effect of RNAi, some insects were sampled for qRT-PCR 3 days after injection. To examine the function of Kr-h1 in ovarian development, female adults were injected with 1 μl of *Kr-h1* or *bla* dsRNA (10 μg/μl) into the head on the day after adult emergence. To examine the efficiency of RNAi, the abdomens of some insects were sampled for qRT-PCR 2 weeks after injection. Their reproductive status was also checked.

Table 1. Sequences of primers.

Gene	Primer	Sequence (5′ >> 3′)
For qRT-PCR		
Kr-h1	krh1-4F	GCC TAG CCA AGA ACT AGA AGA C
	krh1-4R	TCG TTC CAT AGA CTT GAG GAT TG
EF1α	EF1α-F	CCT GCA TCC GTT GCT TTT GT
	EF1α-R	GGC ATC GAG GGC TTC AAT AA
CP-α	CP-α-F	GTT TCA AAG GCT GGT CGC TG
	CP-α-R	GAT CCA CCG CAA GCA ATG TC
Vg-1	Vg-1-F	AGC TAC AAG ACT GAG CAC AAT T
	Vg-1-R	TGC AAC ATT CAC TTC CTG GG
For dsRNA synthesis		
Kr-h1	krh1-2F	CAA GAC CTT CAT CCA GAG TGG
	krh1-2T7F	TAA TAC GAC TCA CTA TAG GCA AGA CCT TCA TCC AGA GTG G
	krh1-2R	GTC GGA GTT TCG AGT ACG TGT
	krh1-2T7R	TAA TAC GAC TCA CTA TAG GGT CGG AGT TTC GAG TAC GTG T
Bla	pBla-F1	TCG CCG CAT ACA CTA TTC TC
	pBlaT7-F	TAA TAC GAC TCA CTA TAG GGA GAC CAC GTC GCC GCA TAC ACT ATT CTC
	pBla-R1	TAC GAT ACG GGA GGG CTT AC
	pBlaT7-R	TAA TAC GAC TCA CTA TAG GGA GAC CAC GTA CGA TAC GGG AGG GCT TAC

Quantitative reverse transcription PCR

To verify the effect of knockdown by RNAi, we measured relative transcript levels by quantitative reverse transcription PCR (qRT-PCR) analysis using FastStart Essential DNA Green Master (Roche, Mannheim, Germany) and the LightCycler 96 system (Roche) followed by cDNA synthesis. The primers used in qRT-PCR are listed in Table 1. *Elongation factor 1-α* (*EF1α*) was used as a control gene for normalization (Futahashi et al., 2013). In all of the reactions, the generation of only a single expected amplicon was confirmed by performing a melting curve analysis. Quantification of cDNAs was performed using a standard curve methodology. All of the qRT-PCR reactions were performed using two technical replicates and at least three biological replicates.

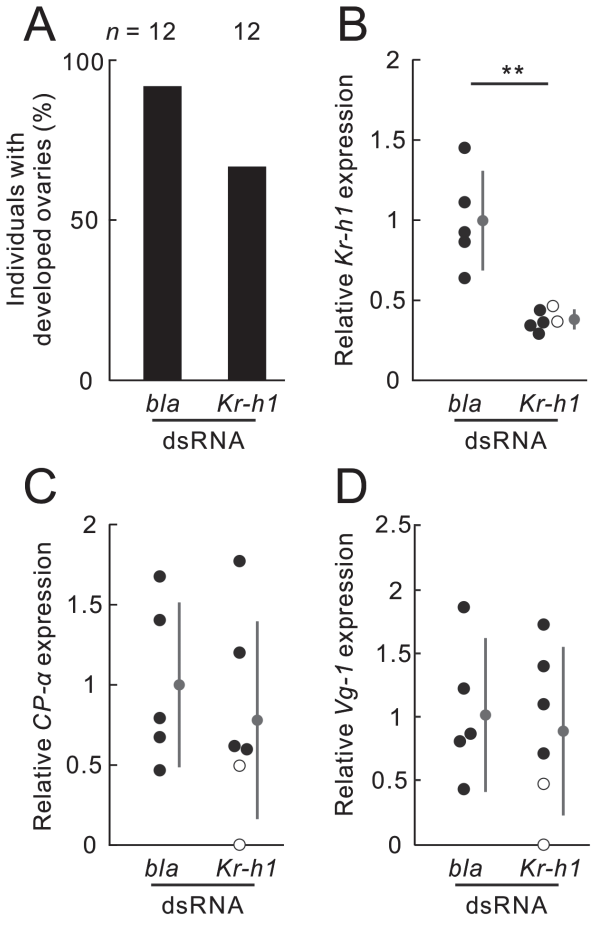

Fig. 1. Effects of *Kr-h1* dsRNA-injection on ovarian development and *Kr-h1*, *cyanoprotein-α* (*CP-α*), and *vitellogenin-1* (*Vg-1*) transcript levels in the abdomen of adult *Riptortus pedestris* reared under long-day conditions at 25°C. **(A)** Insects were injected with dsRNA of *bla* or *Kr-h1* on day 1 after adult emergence. The status of the ovary was observed in insects injected with dsRNA of *bla* or *Kr-h1* 2 weeks after injection. The ordinate shows the percentage of individuals with developed ovaries. No significant difference was detected between *bla* dsRNA-injected individuals and *Kr-h1* dsRNA-injected individuals (Fisher's exact test, $P > 0.05$). **(B)** Each plot shows the relative amount of *Kr-h1* mRNA (the ratio to *EF1α* expression) from a single abdomen collected 8 h after light-on (at ZT 8) (n = 5–9). **(C)** The relative transcript levels of *CP-α* from a single abdomen collected at ZT 8 (n = 5–6). Transcript levels of *Kr-h1* in the abdomen of *Kr-h1* dsRNA-injected individuals were significantly lower than those in control individuals (Aspin-Welch t-test, $P < 0.05$). (D) The relative transcript levels of *Vg-1* from a single abdomen collected at ZT 8 (n = 5–6). Open and solid black circles indicate samples from the abdomen of individuals with undeveloped ovaries and developed ovaries, respectively. The mean values of control insects injected with *bla* dsRNA were set at 1.0. The solid gray circles and error bars represent mean values and standard deviations, respectively. There were no significant differences in the transcript levels of *CP-α* or *Vg-1* between insects injected with *bla* dsRNA and those injected with *Kr-h1* dsRNA in the abdomen (Aspin-Welch t-test, $P > 0.05$).

Morphological observation of fifth instar nymphs

To obtain nymphs at the desired age, third instar nymphs were individually housed in a small cup. Whether they ecdysed to fourth instar nymphs was checked during 17:00–20:00 JST every day. In the present study, day 0 is defined as the 24-h period from lights-on of the day of ecdysis, and the next 24-h period is day one. The dorsal side of the whole body of the fifth instar nymphs on day five was photographed using a digital camera (HDCE-10C; AS ONE, Osaka, Japan) attached to a stereomicroscope (S8 APO; Leica Microsystems, Wetzlar, Germany) to observe the wing bud. Some individuals were reared until the next ecdysis. To compare morphology, the others were immersed in 70% ethanol on day five of the fifth instar. Various parts of their body were photographed using a stereomicroscope with an attached digital camera (ISN230; Nikon, Tokyo, Japan). Adults were immersed in 70% ethanol on day five for comparison of the dorsal side of the abdomen. The averaged value of red, green, and blue (RGB; each parameter defines the intensity of the color as an integer between 0 and 255) in the dorsal side of the fifth instar nymph and adult was obtained using NIS Element (Nikon, Tokyo, Japan). The hue angle (H) was calculated from the averaged value of RGB using $H = \arctan(\sqrt{3}(G-B)/(2R-G-B))$. The photos were processed using CombineZP (available at https://combinezp.software.informer.com/) and CorelDRAW X6 (Corel Corporation, Ontario, Canada) for visualization.

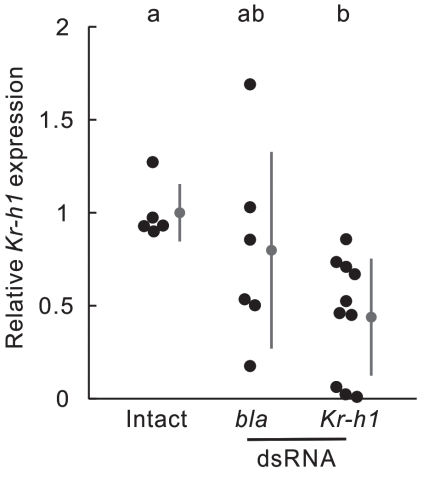

Fig. 2. Effect of *Kr-h1* dsRNA injection on *Kr-h1* transcript level in fourth instar nymphs of *Riptortus pedestris* reared under long-day conditions at 25°C. Fourth instar nymphs were injected with dsRNA of *bla* or *Kr-h1* on day 1. To examine the effect of dsRNA-injection, the nymphs were collected on day four of the fourth instar for qRT-PCR. Each plot shows the relative amount of *Kr-h1* mRNA (the ratio to *EF1α* expression) from a whole-body (n = 5–10). The mean value of intact nymphs was set at 1.0. The solid gray circles and error bars represent mean values and standard deviations, respectively. Injection of *Kr-h1* dsRNA suppressed *Kr-h1* transcript levels by about 50% (*$P < 0.05$, **$P < 0.01$, t-test). The same letters indicate that values are not significantly different (Tukey-type multiple comparisons, $P > 0.05$; Zar, 2010).

Statistical analysis

Statistical analyses were performed using JMP® Pro 14 (SAS Institute Inc., Cary, NC, USA). Fischer's exact test was used for pairwise comparisons of proportions of individuals with developed ovaries. Student's *t*-test or Aspin Welch's *t*-test was used for detecting significant differences in pairwise comparisons of transcript levels of *Kr-h1*, *CP-α*, and *Vg-1*. For comparisons of multiple data, Tukey-type multiple comparisons or Steel-Dwass multiple comparisons were used (Zar, 2010).

RESULTS

Ovarian development

When injected with *bla* dsRNA (control), 92% of females developed ovaries under long-day conditions (Fig. 1A). The ovaries developed in 67% of females injected with dsRNA of *Kr-h1* (Fig. 1A). There was no significant difference between the control and *Kr-h1* dsRNA-injected females. After injection of dsRNA of *Kr-h1*, the expression level of *Kr-h1* in the abdomen decreased to 38% of the level in the abdomen of the control insects (Fig. 1B). To examine the effect of *Kr-h1* knockdown on ovarian development at the level of gene expression, we measured the expression levels of JH-inducible genes *CP-α* and *Vg-1*. There was no significant difference in the expression level of *CP-α* or *Vg-1* in the abdomen between the control and *Kr-h1* dsRNA-injected insects (Fig. 1C, D).

Nymphal morphology

Injection of *Kr-h1* dsRNA decreased the transcript level of *Kr-h1* 3 days after injection when fourth instar nymphs were injected with *Kr-h1* dsRNA on day 1 after the third nymphal ecdysis. The *Kr-h1* transcript level was significantly different from that in intact insects but not from that in *bla* dsRNA-injected insects (Fig. 2). When we injected *Kr-h1* dsRNA into fourth instar nymphs, we found that 84% of nymphs had defective phenotypes in the wing bud after the next ecdysis (Table 2). We defined these nymphs as abnormal fifth instar nymphs and classified their phenotypes of wing bud into four types (Fig. 3A; Table 2) as follows: Type A: Two wing buds are separated by a gap that is smaller than the width of the body. Type B: The wing buds are puffed up. Type C: The wing buds are wrinkled. Type D: Two wing buds are separated by a gap that is larger than the width of the body. In adults, right and left wings overlap each other and reach the tip of the abdomen (Fig. 3B). In intact nymphs, no defects in the wing bud were observed. A few *bla* dsRNA-injected (control) fifth instar nymphs had wing buds of Type A (Table 2), suggesting that injection itself produces Type A wing buds only rarely. We further observed several body parts of the abnormal fifth instar nymphs and found that most of them exhibited at least one typical characteristic of adult morphological features, such as ocelli in the head, the connexivum of the abdomen, or adult genitals (Fig. 3). In *R. pedestris*, adults have two ocelli in their heads and nymphs have no ocelli from the first to fifth (last) instar (Edde, 2021). We found that 84% of the abnormal fifth instar nymphs had ocelli (Fig. 3C; Table 2). Two types of ocelli were observed

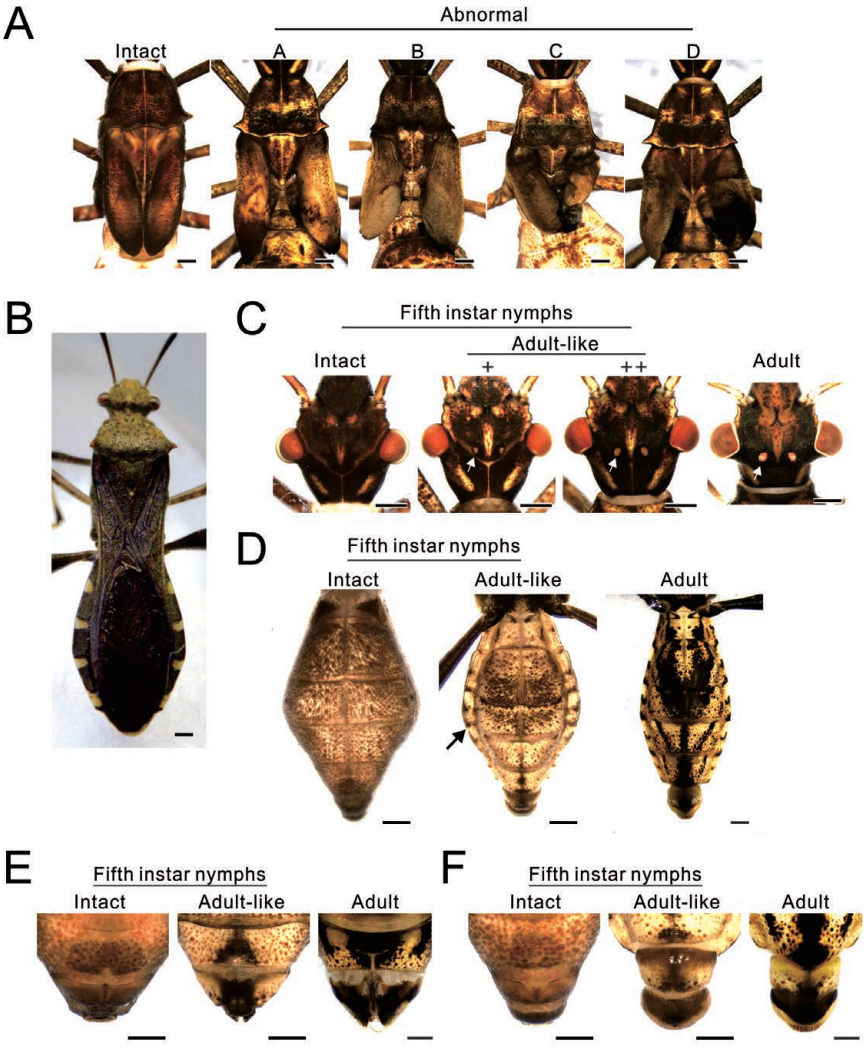

Fig. 3. Effect of *Kr-h1* dsRNA-injection on the external morphology of fifth instar nymphs of *Riptortus pedestris*. The fourth instar nymphs were injected with *bla* or *Kr-h1* dsRNA on day 1 after molting. Scale bar, 500 μm. **(A)** Wing bud of fifth instar nymphs of intact and *Kr-h1* dsRNA-injected nymph. Defective phenotypes of the wing bud in *Kr-h1* dsRNA-injected individuals were classified into four types. Type A: Two wing buds are separated by a gap that is smaller than the width of the body. Type B: The wing buds are puffed up. Type C: The wing buds are wrinkled. Type D: Two wing buds are separated by a gap that is larger than the width of the body. **(B)** The dorsal side of a female adult. The right and left wings overlap each other and reach the tip of the abdomen. **(C)** Head of fifth instar nymph. Intact nymphs did not have two ocelli in the head, whereas some *Kr-h1* dsRNA-injected nymphs had flattened, small ocelli (+), or apparent adult ocelli (++). White arrows show an ocellus in the head. **(D)** Ventral side of the abdomen of fifth instar nymph and adult. Connexivum (marked by an arrow) was observed along the edge of the abdomen in some *Kr-h1* dsRNA-injected nymphs. **(E)** Female genitals in fifth instar nymphs and one adult. **(F)** Male genitals in fifth instar nymphs and one adult.

Table 2. Morphological features in fifth instar nymphs with *Kr-h1* dsRNA-injection in *Riptortus pedestris*.

Treatment	*n*	Wing bud					Adult morphological features						
		Normal	Abnormal				Ocelli			Connexivum		Genitals	
			A	B	C	D	–	+	++	–	+	–	+
Intact	36	36	0	0	0	0	36	0	0	35	1	36	0
bla dsRNA	42	39	3	0	0	0	39	0	0	39	0	42	0
*Kr-h*1 dsRNA	69	11	3	31	19	5	20	22	27	50	19	27	42

See Fig. 3 for the morphology of wing bud in the intact and abnormal fifth instar nymph, and three adult morphological features (ocelli, connexivum, and adult-like genitals).

in the abnormal fifth instar nymphs: ++ (55%) looked the same as the ocelli of adults, while + (45%) were flattened and small (Fig 3C; Table 2). In abnormal fifth instar nymphs, 33% had a connexivum, which is observed along the edge of the abdomen in adults but not in nymphs, although almost no intact nymphs and none of the control nymphs had a connexivum (Fig. 3D; Table 2). Female adults had a cleavage at the abdominal tip, i.e., vulva between the first valvifers, but intact fifth instar nymphs did not have such a structure in the future genitals (Fig. 3E). Male adults had a genital capsule at the genitals, which was not observed in intact fifth instar nymphs (Fig. 3F). In abnormal fifth instar nymphs, however, 72% had adult-like genitals (Fig. 3F, G; Table 2). Most of the fifth instar nymphs with normal wing buds after *Kr-h1* dsRNA-injection had no adult morphological features in the ocelli, connexivum, or genitals. The percentages of individuals with zero to three adult morphological features in the ocelli, connexivum, and genitals were almost the same among Types B, C, and D (see Supplementary Figure S1). This suggests that we can regard Types B, C, and D as an indicator of precocious adult development, even though none of these three types morphologically reproduced adult wings.

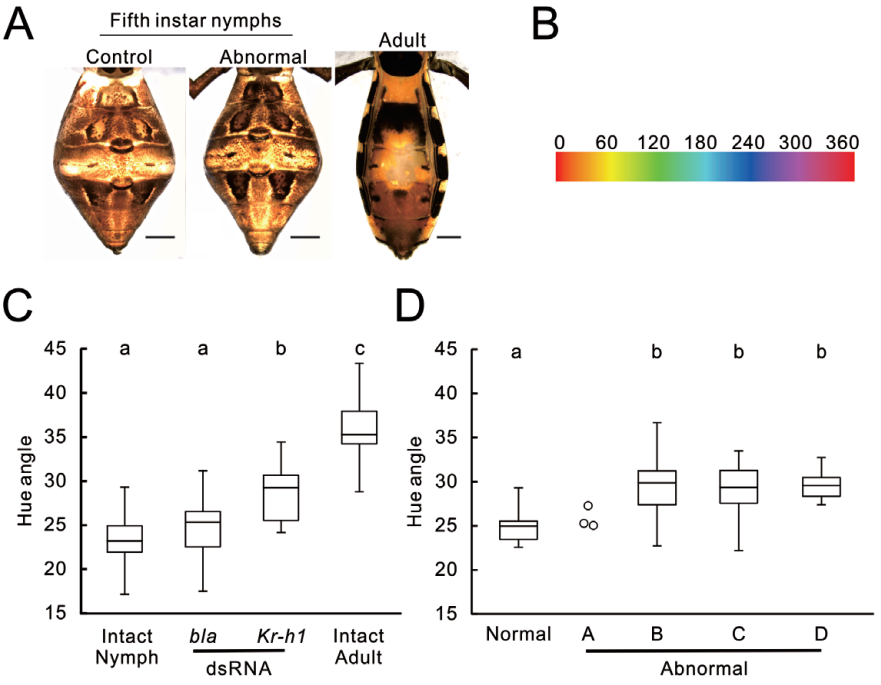

Fig. 4. The body color in the dorsal side of the abdomen of *Riptortus pedestris*. **(A)** The dorsal side of the abdomen of control, abnormal fifth instar nymph with *Kr-h1* dsRNA-injection, and adult of *R. pedestris*. The yellow pattern is observed in the adult abdomen. Scale bar, 1 mm. **(B)** Diagram of hue angle. **(C)** The ordinate shows the hue angle. The hue angle was calculated from RGB averaged in the image of the dorsal area of the abdomen. The hue angle of the dorsal side of the abdomen was approximately 25° in intact nymphs and *bla* dsRNA-injected nymphs. *Kr-h1* dsRNA-injected nymphs and intact adults had 30° and 35° hue angles, respectively. **(D)** The hue of the dorsal side of the abdomen in *Kr-h1* dsRNA-injected nymphs is shown. The same letters indicate that hues are not significantly different (Steel-Dwass multiple comparisons, $P > 0.05$).

Adults have a yellow pattern on the dorsal side of the abdomen under the wings (Fig. 4A), but the nymphs do not. The abnormal fifth instar nymphs with *Kr-h1* dsRNA-injection had a yellow pattern on the dorsal side of the abdomen after ecdysis, although it looked different from that of adults (Fig. 4A). In these abnormal nymphs, there were various yellow patterns, i.e., some individuals had a yellow spot in the central area of the dorsal abdomen, while others had a yellow pattern ranging over the whole abdominal region. To gauge the change of body color, therefore, the hue angle (color phase) of the dorsal side of the abdomen was examined because it was impossible to evaluate color changes with various patterns by using the human eye. Adults with a yellow pattern on the dorsal side of their abdomen had hue angle of approximately 35°. The hue angle of the intact and control fifth instar nymphs was around 25°. Interestingly, the hue angle of abnormal fifth instar nymphs with *Kr-h1* dsRNA-injection was approximately 30°, which was between the values of control nymphs and adults (Fig. 4B). Among *Kr-h1* dsRNA-injected individuals, the abnormal fifth instar nymphs except for Type A exhibited a larger hue angle compared to normal fifth instar nymphs with *Kr-h1* dsRNA-injection (Fig. 4D). There was no significant difference among Types B, C, and D (Fig. 4D).

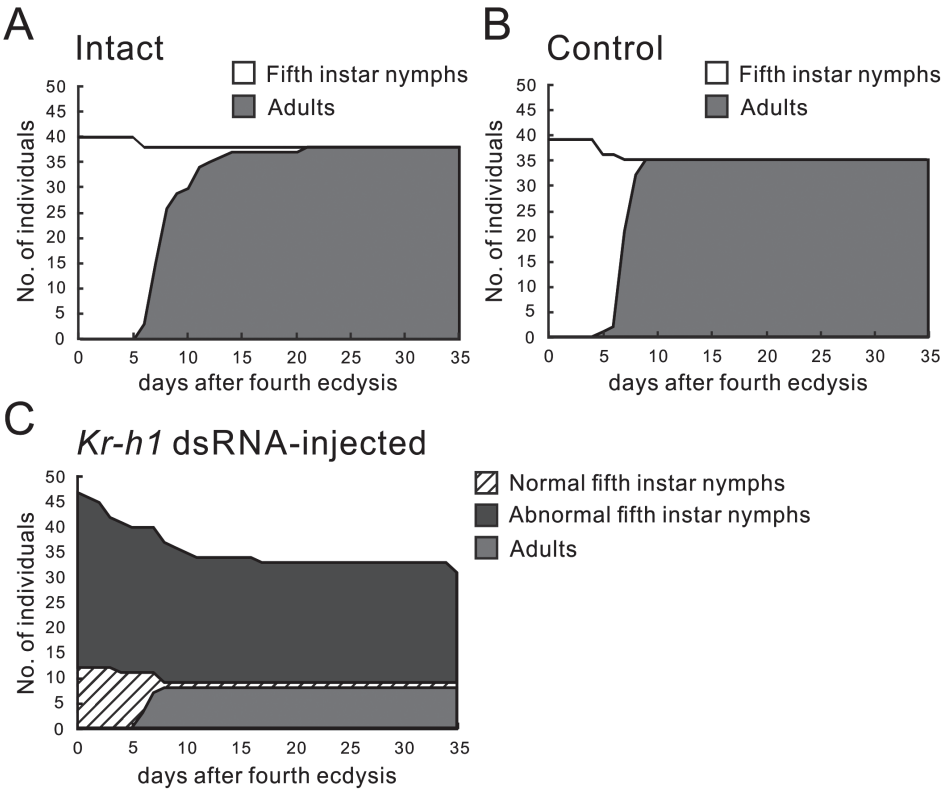

Fig. 5. Nymphal and nymphal-adult ecdyses in intact insects **(A)** and insects injected with **(B)** *bla* or **(C)** *Kr-h1* dsRNA in *Riptortus pedestris* under long-day conditions at 25°C. The dsRNA was injected into the fourth instar nymphs. None of the abnormal fifth instar nymphs that appeared after *Kr-h*1 dsRNA-injection emerged as adults. n = 39–47.

Nymphal-adult ecdysis

More than 90% of intact fifth instar nymphs and all fifth instar nymphs with *bla* dsRNA-injection underwent ecdysis within 11 days after the fourth nymphal ecdysis (Fig. 5A, B). In the *Kr-h1* dsRNA-injected group, 89% of normal fifth instar nymphs molted to adults, while none of the abnormal fifth instar nymphs underwent ecdysis; rather, they survived as fifth instar nymphs for more than 30 days (Fig. 5C).

DISCUSSION

In adult insects, JH promotes vitellogenesis, including Vg synthesis in the fat body and oocyte maturation via the Met/Tai complex (Wu et al., 2021). *Kr-h1* is a JH early-response gene encoding a C_2H_2 zinc-finger type transcription factor that transduces JH signals to regulate reproduction in some insects (Wu et al., 2021) but not in others (Smykal et al., 2014; Gujar and Palli, 2016). The function of Kr-h1 in reproduction varies depending on the insect species. Knockdown of *Met* or *Kr-h1* by RNAi substantially reduced *Vg* expression in the fat body and arrested follicular epithelium development, oocyte maturation, and ovarian growth in *L. migratoria* (Song et al., 2014). Knockdown of *Met* or *Kr-h1* resulted in reduced *Vg* expression and impeded ovarian development with lowered fecundity in *B. dorsalis* (Yue et al., 2018). Similar findings have also been reported in *S. furcifera, N. lugens*, and the red flour beetle, *Tribolium castaneum* (Lin et al., 2015; Jiang et al., 2017; Hu et al., 2019, 2020; Naruse et al., 2020). Sheng et al. (2011) showed that JH additionally regulates *Vg* expression through the insulin-like peptide pathway in *T. castaneum*. In contrast, knockdown of *Met* or *Tai*, but not *Kr-h1,* reduced *Vg* expression and blocked ovarian development in *P. apterus* (Smykal et al., 2014). Similarly, knockdown of *Met* or *Tai* affected *Vg* expression and fecundity, whereas knockdown of *Kr-h1* did not, in *C. lectularius* (Gujar and Palli, 2016).

Recently, we have shown that *Kr-h1* is one of the JH-inducible genes in *R. pedestris* (Dong et al., 2021). To clarify whether Kr-h1 functions in ovarian development, we tried knockdown of *Kr-h1* by RNAi. The results showed that knockdown of *Kr-h1* caused an approximately 25% reduction in the percentage of individuals with developed ovaries (Fig. 1A), but did not provide a clear answer because the efficiency of RNAi was not sufficient: *Kr-h1* transcript levels decreased 50% in the abdomen (Fig. 1B). Technical improvement of RNAi would help to further our understanding of the function of Kr-h1 in the adults of *R. pedestris* in future studies. To complement the present results obtained by RNAi, we examined the expression levels of *CP-*α and *Vg-1* in *Kr-h1* dsRNA-injected females. *CP-*α and *Vg-1* are JH-inducible genes and involved in female reproduction (Miura et al., 1991; Hirai et al., 1998; Ikeno et al., 2010; Lee et al., 2017). There was no effect of *Kr-h1* knockdown on transcript levels of *CP-*α or *Vg-1* in the abdomen (Fig. 1C, D). Further investigations are necessary to elucidate the function of Kr-h1 in female reproduction in *R. pedestris*. Kr-h1 of *R. pedestris* has high similarity to Kr-h1 of *P. apterus* and *C. lectularius* (Heteroptera, Hemiptera), whose ovarian development, including the *Vg* transcript level, is not affected by knockdown of *Kr-h1* (Smykal et al., 2014; Gujar and Palli, 2016; Dong et al., 2021). In *N. lugens* and *S. furcifera*, which belong to a different suborder than *R. pedestris*, Auchenorrhyncha in Hemiptera, interestingly, Kr-h1 plays a pivotal role in female reproduction (Lin et al., 2015; Jiang et al., 2017; Hu et al., 2019, 2020). Kr-h1 of heteropteran insects may play a minor or no such role. This should be addressed in future studies.

The hemimetabolous insects have several nymphal instars followed by nymphal-adult ecdysis. These processes are regulated by JH and molting hormone (ecdysteroid). JH maintains the larval (nymphal) state of insects by modulating the cellular responses to the ecdysteroid during each molting. A drastic decrease in JH in the final instar leads to an ecdysteroid spike to induce the metamorphic molt (Jindra et al., 2013). Kr-h1 acting downstream of JH controls larval

metamorphosis (Kayukawa et al., 2012, 2017). To elucidate the function of Kr-h1 in metamorphosis in *R. pedestris*, we performed knockdown of *Kr-h1* by RNAi in fourth instar nymphs. The results showed that RNAi of *Kr-h1* was efficient in nymphs (Fig. 2), although the transcript levels of *Kr-h1* varied among individuals, suggesting that RNAi was not effective for all of the individuals tested. This variability of the effects of RNAi may have resulted in the variety of morphological features observed in *Kr-h1* dsRNA-injected abnormal fifth instar nymphs (Fig. 3; Table 2). In several insect species, *Kr-h1* RNAi caused precocious development of adult features such as wings, genitals, and body color (Konopova et al., 2011; Lozano and Belles, 2011; Ishimaru et al., 2019). In the present study, the most dominant phenotype appeared as abnormalities in the wing bud in *Kr-h1* dsRNA-injected individuals (Table 2). Consistent with previous reports, we also observed several adult features, including ocelli, connexivum, genitals, and the color of the dorsal side of the abdomen in abnormal fifth instar nymphs with *Kr-h1* dsRNA-injection in *R. pedestris*. These results suggest that downregulation of *Kr-h1* caused precocious adult development in *R. pedestris*. To our knowledge, this is the first report showing that ocelli formation was observed in *Kr-h1* RNAi-treated nymphs (Fig. 3C). We did not examine the internal structure or function of the ocelli. The abnormal fifth instar nymphs of *Kr-h1* RNAi-treated nymphs did not emerge as adults for over 1 month (Fig. 5). A similar result was reported in *G. bimaculatus*, i.e., knockdown of *Kr-h1* by RNAi caused adult morphological features and failure to undergo ecdysis (Ishimaru et al., 2019).

In conclusion, the present study demonstrated that Kr-h1 is involved in maintaining the nymphal state. In contrast, the function of Kr-h1 in ovarian development remains unclear in the adult of *R. pedestris*. In the present study, we focused only on the functions of Kr-h1 in nymph-adult transition and reproduction in female adults. Several studies reported that dramatic metamorphosis is precisely regulated by the mutual regulation of transcription factors Kr-h1, Broad-Complex (Br), and ecdysone-induced protein 93 (E93) (e.g., see Ureña et al., 2016). The effects of downregulation of *Kr-h1* on *Br* and *E*93 expression and the effects of downregulation of *Br* and *E*93 on *Kr-h1* expression in *R. pedestris* are interesting issues to be addressed in future studies.

ACKNOWLEDGMENTS

We thank Teiji Sota for allowing us to use the LightCycler 96 system. We also thank Elizabeth Nakajima for proofreading the manuscript. This work was supported by JSPS KAKENHI (Grant-in-Aid for Scientific Research B, Grant Number 18H02478) to HN.

COMPETING INTERESTS

The authors declare that they have no conflicts of interest.

AUTHOR CONTRIBUTIONS

HN and CI designed the study. LD, NM, and CI performed the experiments and analyzed the data. LD, HN, and CI wrote the manuscript, and all authors approved the final version of the manuscript.

SUPPLEMENTARY MATERIALS

Supplementary material for this article is available online. (URL: https://doi.org/10.2108/zs220025)

Supplementary Figure S1. The proportion of individuals with zero to three adult morphological features (ocelli, connexivum, and adult-like genitals) in normal and abnormal fifth instar nymphs with *Kr-h1* dsRNA-injection in *Riptortus pedestris*.

REFERENCES

Dong L, Udaka H, Numata H, Ito C (2021) Regulation of *Krüppel homolog* 1 expression by photoperiod in the bean bug, *Riptortus pedestris.* Physiol Entomol 46: 82–93

Edde PA (2021) Field Crop Arthropod Pests of Economic Importance. 1st ed, Academic Press, Cambridge, MA

Futahashi R, Tanaka K, Tanahashi M, Nikoh N, Kikuchi Y, Lee BL, et al. (2013) Gene expression in gutsymbiotic organ of stinkbug affected by extracellular bacterial symbiont. PLOS ONE 8: e64557

Gujar H, Palli SR (2016) Juvenile hormone regulation of female reproduction in the common bed bug, *Cimex lectularius*. Sci Rep 6: 35546

Hafeez A, Li B, Atiq MN, Wang X-P (2020) Developmental differences on the internal reproductive systems between the prediapause and prereproductive *Riptortus pedestris* adults. Insects 11: 347

Hirai M, Yuda M, Shinoda T, Chinzei Y (1998) Identification and cDNA cloning of novel juvenile hormone responsive genes from fat body of the bean bug, *Riptortus clavatus* by mRNA differential display. Insect Biochem Mol Biol 28: 181–189

Hu K, Tian P, Yang L, Qiu L, He H, Ding W, et al. (2019) Knockdown of *Methoprene-Tolerant* arrests ovarian development in the *Sogatella furcifera* (Hemiptera: Delphacidae). J Insect Sci 19: 5

Hu K, Tian P, Yang L, Tank Y, Qiu L, He H, et al. (2020) Molecular characterization of the Krüppel-homolog 1 and its role in ovarian development in *Sogatella furcifera* (Hemiptera: Delphacidae). Mol Biol Rep 47: 1099–1106

Ikeno T, Tanaka SI, Numata H, Goto SG (2010) Photoperiodic diapause under the control of circadian clock genes in an insect. BMC Biol 8: 116

Ishimaru Y, Tomonari S, Watanabe T, Noji S, Mito T (2019) Regulatory mechanisms underlying the specification of the pupal-homologous stage in a hemimetabolous insect. Phil Trans R Soc B 374: 20190225

Jiang J, Xu Y, Lin X (2017) Role of *Broad-Complex* (*Br*) and *Krüppel homolog 1* (*Kr-h1*) in the ovary development of *Nilaparvata lugens*. Front Physiol 8: 1013

Jindra M, Palli SR, Riddiford LM (2013) The juvenile hormone signaling pathway in insect development. Annu Rev Entomol 58: 181–204

Jindra M, McKinstry WJ, Nebl T, Bittova L, Ren B, Shaw J, et al. (2021) Purification of an insect juvenile hormone receptor complex enables insights into its post-translational phosphorylation. J Biol Chem 297: 201387

Kamano S (1991) *Riptortus clavatus* (Thunberg) (bean bug). In "Rearing Methods of Insects" Ed by T Yushima, S Kamano, Y Tamaki, Japan Plant Protection Association, Tokyo, pp 46–49 (in Japanese)

Kayukawa T, Minakuchi C, Namiki T, Togawa T, Yoshiyama M, Kamimura M, et al. (2012) Transcriptional regulation of juvenile hormone-mediated induction of Krüppel homolog 1, a repressor of insect metamorphosis. Proc Natl Acad Sci USA 109: 11729–11734

Kayukawa T, Jouraku A, Ito Y, Shinoda T (2017) Molecular mechanism underlying juvenile hormone-mediated repression of precocious larval-adult metamorphosis. Proc Natl Acad Sci USA 114: 1057–1062

Konopova B, Smykal V, Jindra M (2011) Common and distinct roles of juvenile hormone signaling genes in metamorphosis of holometabolous and hemimetabolous insects. PLOS ONE 6: e28728

Lee JB, Park K-E, Lee SA, Jank SH, Eo HJ, Jang HA, et al. (2017) Gut symbiotic bacteria stimulate insect growth and egg production by modulating hexamerin and vitellogenin gene expression. Dev Comp Immunol 69: 12–22

Lin X, Yao Y, Wang B (2015) *Methoprene-tolerant* (*Met*) and *Krüppel-homolog 1* (*Kr-h1*) are required for ovariole development and egg maturation in the brown plant hopper. Sci Rep 5: 18064

Lozano J, Belles X (2011) Conserved repressive function of Krüppel homolog 1 on insect metamorphosis in hemimetabolous and holometabolous species. Sci Rep 1: 163

Minakuchi C, Namiki T, Shinoda T (2009) *Krüppel homolog 1*, an early juvenile hormone-response gene downstream of *Methoprene-tolerant*, mediates its anti-metamorphic action in the red flour beetle *Tribolium castaneum*. Dev Biol 325: 341–350

Miura K, Chinzei Y, Shinoda T, Numata H (1991) Cyanoprotein: quantitative changes and synthesis in diapause and juvenile hormone analog treated bean bug, *Riptortus clavatus*. Insect Biochem 21: 553–562

Naruse S, Washidu Y, Miura K, Shinoda T, Minakuchi C (2020) *Methoprene-tolerant* is essential for embryonic development of the red flour beetle *Tribolium castaneum*. J Insect Physiol 121: 104017

Numata H, Hidaka T (1982) Photoperiodic control of adult diapause in the bean bug, *Riptortus clavatus* Thunberg (Heteroptera: Coreidae). I. Reversible induction and termination of diapause. Appl Entomol Zool 17: 530–538

Numata H, Hidaka T (1984) Termination of adult diapause by a juvenile hormone analogue in the bean bug, *Riptortus clavatus*. Zool Sci 1: 751–754

Raikhel AS, Deitsch KW, Sappington TW (1997) Culture and analysis of the insect fat body. In "The Molecular Biology of Insect Disease Vectors" Ed by JM Crampton, CB Beard, C Louis, Springer, Dordrecht, pp 507–522

Roy S, Saha TT, Zou Z, Raikhel AS (2018) Regulatory pathways controlling female insect reproduction. Annu Rev Entomol 63: 489–511

Sheng Z, Xu J, Bai H, Zhu F, Palli SR (2011) Juvenile hormone regulates vitellogenin gene expression through insulin-like peptide signaling pathway in the red flour beetle, *Tribolium castaneum*. J Biol Chem 286: 41924–41936

Smykal V, Bajgar A, Provaznik J, Fexova S, Buricova M, Takaki K, et al. (2014) Juvenile hormone signaling during reproduction and development of the linden bug, *Pyrrhocoris apterus*. Insect Biochem Molec Biol 45: 69–76

Song J, Wu Z, Wang Z, Deng S, Zhou S (2014) Krüppel-homolog 1 mediates juvenile hormone action to promote vitellogenesis and oocyte maturation in the migratory locust. Insect Biochem Molec Biol 52: 94–101

Ureña E, Chafino S, Manjón C, Franch-Marro X, Martín D (2016) The occurrence of the holometabolous pupal stage requires the interaction between E93, Krüppel-homolog 1 and broad-complex. PLoS Genet 12: e1006020

Wu Z, Yang L, He Q, Zhou S (2021) Regulatory mechanisms of vitellogenesis in insects. Front Cell Dev Biol 8: 593613

Yue Y, Yang R-L, Wang W-P, Zhou Q-H, Chen E-H, Yuan G-R, et al. (2018) Involvement of *Met* and *Kr-h1* in JH-mediated reproduction of female *Bactrocera dorsalis* (Hendel). Front Physiol 9: 482

Zar JH (2010) Biostatistical Analysis. 5th ed, Prentice Hall, Upper Saddle River, NJ

(Received March 6, 2022 / Accepted July 28, 2022 /
Published online September 27, 2022)